Available online at www.sciencedirect.com
ScienceDirect
Trans. Nonferrous Met. Soc. China 35(2025) 788−799
Transactions of Nonferrous Metals Society of China
www.tnmsc.cn

Comparison of edge crack behavior of Mg−3Al−1Zn sheets rolled from as-cast, as-rolled and as-extruded alloys

Qiu-yan SHEN[1,2], Shang-yi ZHANG[1,2], Qiang LIU[1,2],
Jiang-feng SONG[1,2,3], Dong-xia XIANG[4], Bin JIANG[1,2,3], Fu-sheng PAN[1,2,3]

1. National Engineering Research Center for Magnesium Alloys, Chongqing University, Chongqing 400044, China;
2. College of Materials Science and Engineering, Chongqing University, Chongqing 400044, China;
3. National Key Laboratory of Advanced Casting Technologies, Chongqing University, Chongqing 400044, China;
4. Chongqing Advanced Light Metal Research Institute, Chongqing 400044, China

Received 12 August 2023; accepted 25 April 2024

Abstract: Edge cracking is one of the most serious problems in the rolling process of magnesium alloy sheets, which limits its application. In this work, the edge cracking behavior of different initial AZ31 alloy sheets, including as-cast (AC), as-rolled (AR) and as-extruded (AE), was systematically investigated and compared under the online heating rolling (O-LHR) process with a single-pass reduction of 50% at 250 °C. The results show that both AC and AR sheets exhibit severe edge cracking behavior after the O-LHR. Among them, the AR sheet exhibits the severest edge cracking behavior on the rolling plane (RD−TD) and longitudinal section (RD−ND), which is attributed to the strong basal texture and extremely uneven microstructure with shear bands. While no visible edge crack appears in the AE rolled sheet, which is mainly related to the tilted texture and the more dynamic recrystallization during rolling process. Moreover, it is also found that the micro-cracks of the AC rolled sheet are mainly generated in the local fine-grained area and the twins where recrystallization occurs. In the AR rolled sheet, micro-cracks mainly develop inside the shear bands. Meanwhile, the micro-crack initiation mechanism of AC and AR rolled sheets was also discussed.
Key words: AZ31 sheet; edge crack behavior; initial state; texture; microstructure

1 Introduction

Magnesium (Mg) alloys attracted more and more attention in the fields of aerospace, automotive industry and 3C electronic because of low density, high specific strength, and excellent damping capacity [1−3]. However, Mg alloys exhibit poor ductility and formability at room temperature. This is mainly due to its hexagonal close packed (HCP) crystal structure, which can only activate limited number of independent slip systems at low temperatures [4]. It is well accepted that the rolling process is normally utilized to manufacture the Mg alloy sheets because of the high production efficiency and simple process. However, large amounts of edge cracks often appear in the rolling process of Mg alloy sheets. The occurrence of edge cracks will cause the trimming operation of sheet and leads to a decrease in the productivity, which further restrict its commercial applications. Therefore, it is of great importance to understand the mechanism of edge cracks and finally obtain a method to eliminate edge cracks.

Intensive studies on edge crack behavior have been conducted by researchers using AZ31 sheets with different states. JIA et al [5] performed the

Corresponding author: Qiang LIU, Tel: +86-13320241834, E-mail: q.liu@cqu.edu.cn;
Jiang-feng SONG, Tel: +86-18223616225, E-mail: Jiangfeng.song@cqu.edu.cn
DOI: https://doi.org/10.1016/S1003-6326(24)66714-2

rolling experiment at temperatures ranging from 200 to 400 °C using the as-cast AZ31B magnesium alloy slab ingot as the initial material. They found that the edge cracks were significantly reduced with the increase of rolling temperature, and in the plate at 400 °C only minor edge damage appeared. DING et al [6] also investigated the effects of rolling reduction on the microstructure and edge crack in the as-casted AZ31B magnesium alloys. The results indicated that edge cracks appeared when the total reduction reached 37% at the rolling temperature of 350 °C. In addition, GUO et al [7] studied the influence of rolling speed on the microstructure and mechanical properties of the as-rolled AZ31 alloy sheets by large strain hot rolling. The study revealed that the edge crack behavior was greatly improved with the increase of rolling speed. When the rolling speed exceeded 9.8 m/min, no obvious edge cracks appeared in the sheets. TIAN et al [8] also compared the edge crack behavior of as-rolled AZ31 alloy sheets using width-limited rolling (WLR) and free rolling (FR). They found that the WLR could significantly improve the edge crack behavior of the as-rolled AZ31 alloy sheet. JI et al [9] used the AZ31 alloy sheet with edge curve to carry out cross-variable thickness rolling. It was pointed out that optimizing the edge curve of Mg alloy sheets could provide a theoretical basis for improving the edge cracks. In our previous work [10], it was observed that there were no obvious edge cracks of the extruded AZ31 alloy sheet at rolling temperature of 250 °C during the online heating rolling (O-LHR) process. However, few researchers have focused on comparing the edge cracking behavior of AZ31 alloy sheets with different initial states during the rolling process.

Therefore, in this study, the edge cracking behavior differences of AZ31 alloy sheets with different initial states were studied and compared using the O-LHR. Some interesting and valuable results were obtained, which might provide guidance for the production of Mg alloy sheets and further promote their development and application.

2 Experimental

The initial materials used in this study are commercially available AZ31 magnesium alloy sheets with a thickness of 5 mm. The sheets include the as-cast (AC), as-extruded (AE) and as-rolled (AR) sheets, which corresponds to three Mg sheets with different initial states before rolling. Prior to the rolling process, all the sample sheets were cut into the size of 600 mm in length and 105 mm in width. The optical microstructure at the edge of three different initial sheets is shown in Fig. 1. It is evident that the microstructure in the AC sheet consists of coarse grains. In the AE sheet, the microstructure is inhomogeneous, and large and small grains coexist. The AR sheet exhibits a uniform microstructure.

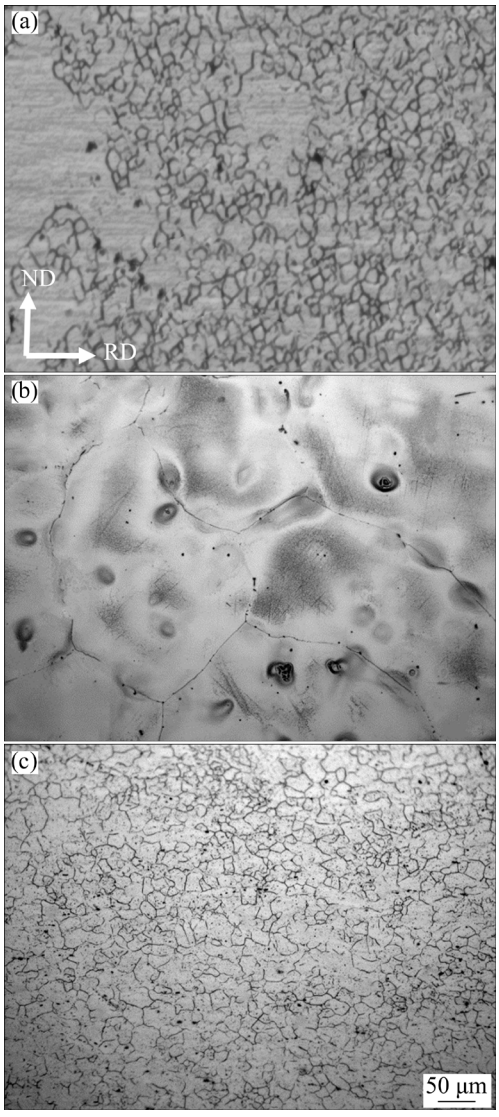

Fig. 1 OM images of different initial sheets: (a) AE; (b) AC; (c) AR

These sheets were rolled at rolling temperature of 250 °C in a single pass through online heating rolling device, the rolling reduction was 50%, the rolling speed was 0.09 m/s, and the rolling tension was 2 kN. The rolling device consists of four rollers

with work rollers of *d*120 mm and support rollers of *d*320 mm. The schematic diagram of the rolling device is shown in Fig. 2. Before the rolling, the rollers were preheated by heating oil. During the rolling, the sheets were heated to the setting temperature by electric current, and rolling tensions were applied at the both ends of sheets to ensure the straightness of the rolled sheets.

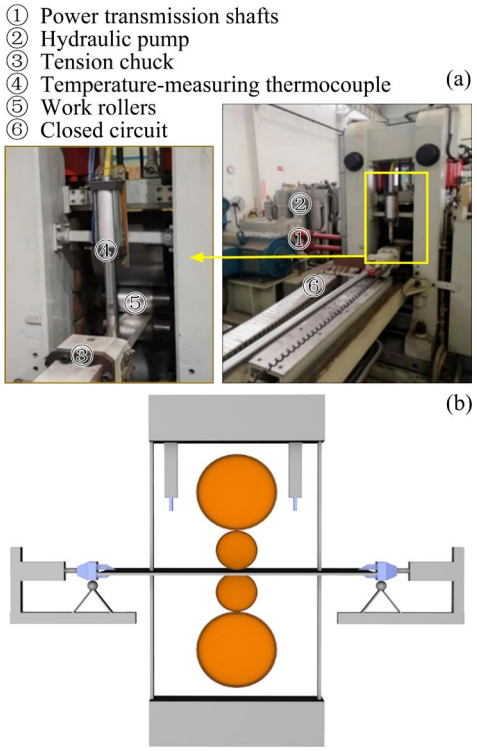

Fig. 2 Equipment diagram (a) and schematic diagram (b) of on-line heating rolling device

After rolling, the crack number, maximum and average crack depths were measured by digital caliper on the rolling direction (RD)−transverse direction (TD) section and RD−normal direction (ND) section of the rolled sheets. The microstructure at the edge of rolled sheets was characterized by optical microscope (OM) and field emission scanning electron microscope (SEM), and electron backscattered diffraction (EBSD). Moreover, the macro-texture at the edge of sheets before and after rolling was examined by X-ray diffraction (XRD). Samples for microstructure observation were taken from the center of sheet on the RD−ND plane. The specimens for OM and SEM observation were initially ground using sand papers ranging from 400# to 2000# grit, and then were chemically etched in an acetic picric solution. Samples for the EBSD experiment were prepared by electric-polishing with AC2 solution using a voltage of 20 V for 80 s at a temperature of −20 °C. The grain orientation characterization was carried out using the field emission scanning electron microscope equipped with the EBSD system at an operating voltage of 20 kV.

3 Results

3.1 Macro-morphology of different AZ31 rolled sheets

Figure 3 shows the macro-morphology and statistical diagram of edge cracks on the RD−TD and RD−ND sections of the rolled sheets with different initial states after rolling. There are no obvious cracks appearing at the edge of the AE rolled sheet, while large amounts of edge cracks are generated in AC and AR rolled sheets (Fig. 3(a)). Moreover, the maximum crack number (within 100 mm), maximum crack depth and average crack depth on the RD−TD section after rolling are shown in Fig. 3(b). The AR sheets show the severest edge cracking behavior. After the O-LHR process, no visible macro-cracks are observed on the longitudinal section (RD−ND) of the AE rolled sheet, while the AC and AR rolled sheets exhibit obvious “V”-shaped or “/”-shaped cracks on the RD−ND section, as illustrated by red dotted lines in Fig. 3(c). According to the statistics, the number of “V”-shaped cracks in the AC rolled sheet within 300 mm is approximately equal to that of “/”-shaped cracks, while the number of “V”-shaped cracks in the AR rolled sheet is much lower than that of “/”-shaped cracks. Furthermore, the AR rolled sheet also exhibits the largest average crack number on the RD−ND section, as shown in Fig. 3(d). This also suggests that compared with the AE and AC sheets, the AR sheet has the worst online heating rolling performance.

3.2 Microstructure of different AZ31 rolled sheets

Figure 4 shows the optical microstructure of sheets with different initial states after rolling. The microstructure of the AE rolled sheet becomes relatively uniform, but a few coarse grains remain. In the AC rolled sheet, many twins are generated inside the original coarse grains to coordinate deformation, leading to an extremely inhomogeneous microstructure, as shown in Fig. 4(b). This is consistent with the work of PEI et al [11]. Meanwhile, some

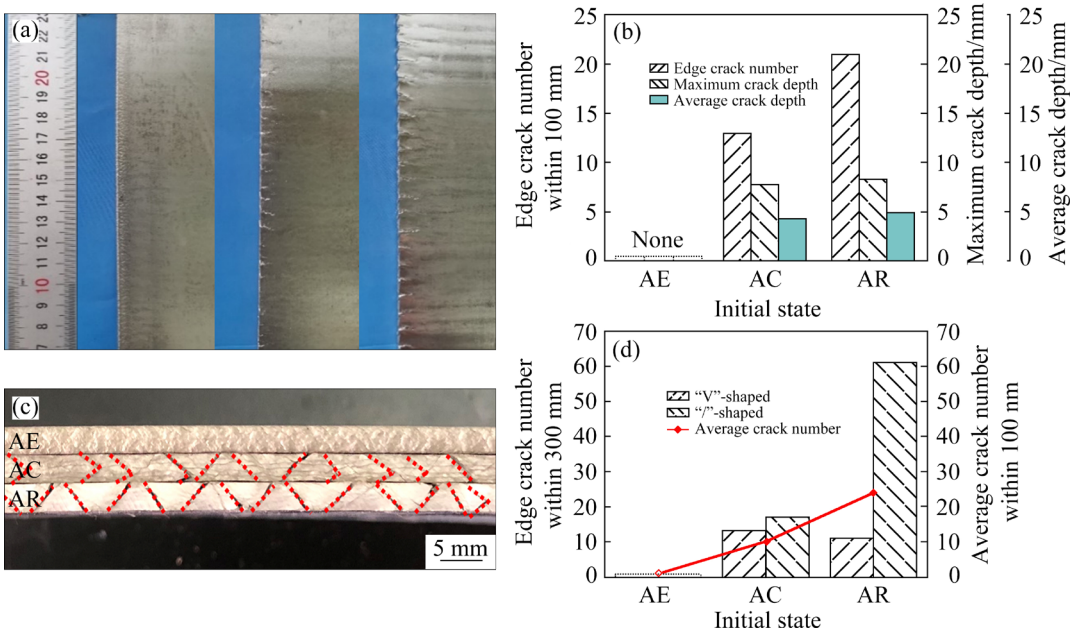

Fig. 3 Macro-morphologies (a, c) and statistical diagrams (b, d) of edge cracks of AZ31 sheets with different initial states after rolling: (a, b) On RD−TD section; (c, d) On RD−ND section

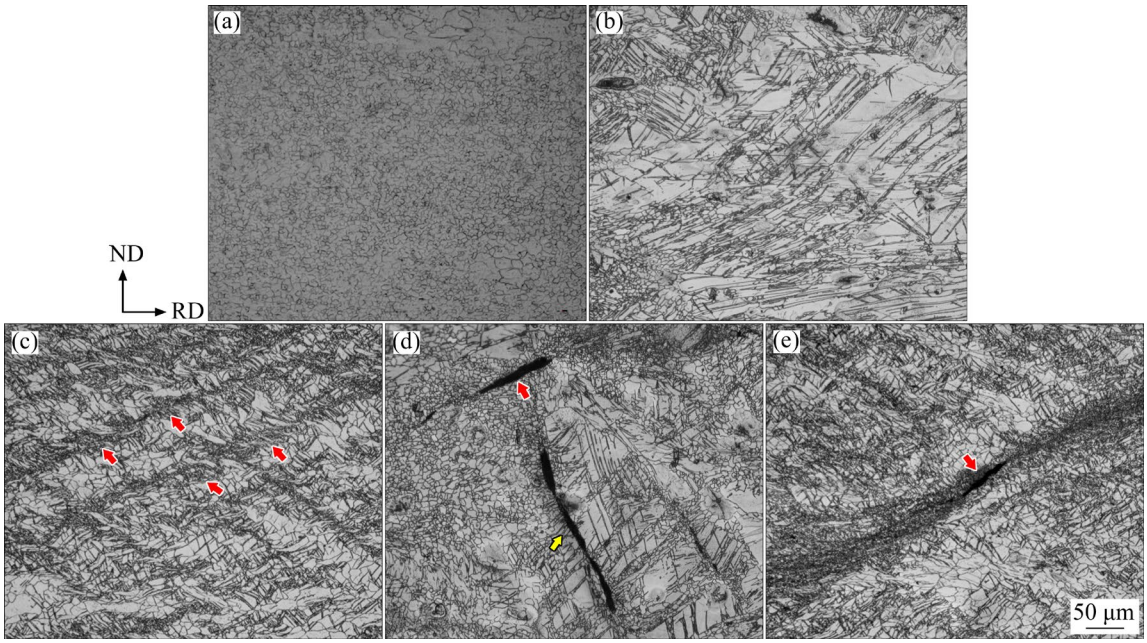

Fig. 4 Metallographic microstructures (a−c) and micro-cracks (d, e) at edge of AZ31 sheets with different initial states after rolling: (a) AE; (b, d) AC; (c, e) AR

fine-grained regions are also found, mainly caused by local recrystallization. For the AR rolled sheet, the microstructure is uneven due to the appearance of large numbers of twins and fine-grained strip bands (highlighted with red arrows in Fig. 4(c)). It was reported that these fine-grained strips were defined as shear bands [12]. Figures 4(d) and (e) show the microstructures in the area that contains micro-cracks at the edge of the AC and AR rolled sheets, respectively. The micro-cracks are mainly initiated inside the fine-grained region (shown by the red arrow in Fig. 4(d)) and the region contains profuse twins (indicated by the yellow arrow in Fig. 4(d)) in the AC rolled sheet. While the micro-crack in the AR rolled sheet is located inside the fine-grained shear bands, as illustrated by the

red arrow in Fig. 4(e).

Figure 5 shows the secondary phase particles distribution at the edge of the rolled sheets with different initial states. The secondary phase particles with both rod and polygonal morphologies of the AC rolled sheet remain relatively coarse. Combined with the mapping results and Ref. [13], these rod- and polygonal-shaped particles are mainly identified as Al−Mn phase, which can be commonly found in Mg−Al-based alloy [14]. The Al−Mn secondary phase particles in the AC rolled sheet are fragmented into several parts due to the large rolling force applied during rolling. As a result, micro-voids are generated inside these coarse Al−Mn phase particles, as marked by the yellow arrows in Fig. 5(b). It is well accepted that the micro-voids are conducive to the initiation of micro-cracks, and similar phenomenon was also found by BAEK et al [15]. The secondary phase particles of AE and AR rolled sheets are fine and diffusely distributed, and are not easy to initiate micro-voids during the rolling process.

The microstructures of rolled sheets with different initial states are obtained, as shown in Fig. 6. It is found that the local coarse grains in the AE rolled sheet are refined, and the microstructure contains a small number of twins (mainly extension twins). It should be noted that almost all fine grains in the microstructure are recrystallized grains. The high degree of recrystallization reduces the geometrically necessary dislocations (Fig. 6(d)), leading to lower stress concentration and more uniform deformation. For the AC rolled sheet, profuse twins are generated inside the original coarse grains, and these twins are commonly referred to as double twins. Part of these twins have undergone twin-induced recrystallization and developed into localized fine grains (Fig. 6(g)), leading to a low degree of recrystallization. In addition, more geometric dislocations accumulate inside some twins and original grains (Fig. 6(h)), leading to an extremely uneven deformation. There is uneven microstructure in the AR rolled sheet due to the occurrence of shear band (Fig. 6(i)). The formation mechanism of shear bands varies with process conditions and material characteristics [16]. Besides, it is shown that the shear band is inclined at an angle relative to the rolling direction, which is mainly related to the shear stress. RAO et al [17] pointed out that shear stress resulted from the compressive stress and the friction force, which led to stress concentration and promoted dynamic recrystallization nucleation in this direction. Compared with the AC and AE rolled sheets, the AR rolled sheet develops pronounced shear bands after rolling (Fig. 4(c)), mainly attributed to the strong basal texture before rolling. WANG et al [18] also found the formation of shear band in Mg−6Zn−0.5Zr alloy plate with basal texture. FATEMI-VARZANEH et al [19] reported that the shear bands caused by strain localization were an important mode of inhomogeneous deformation. This indicates that the deformation of the AR sheet is uneven during the rolling process.

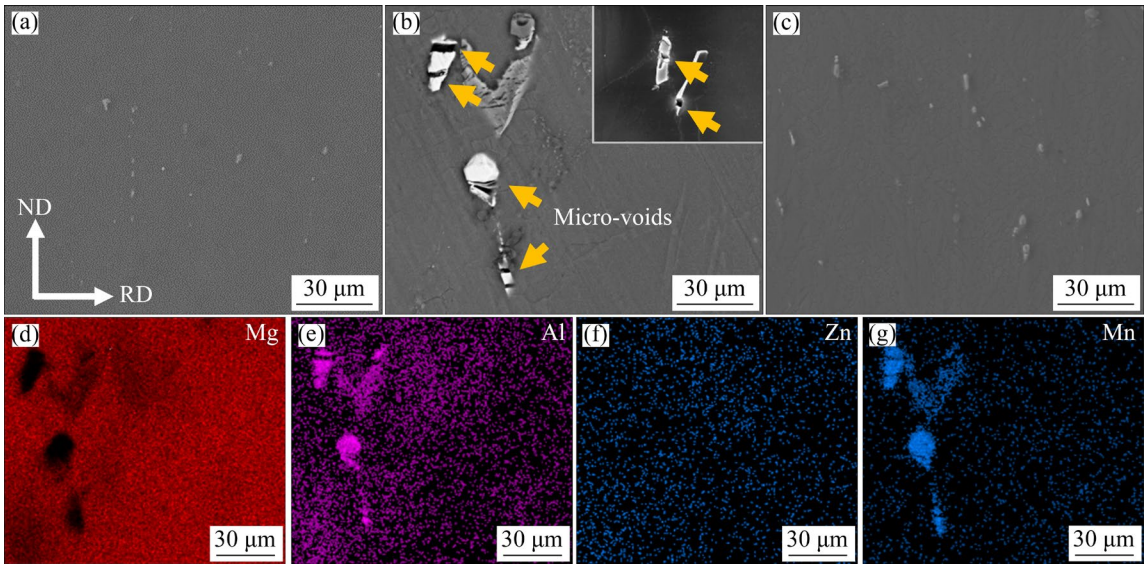

Fig. 5 Secondary phase particles distribution at edge of AZ31 sheets with different initial states after rolling: (a) AE; (b) AC; (c) AR; (d−g) Element distribution scanning maps of (b)

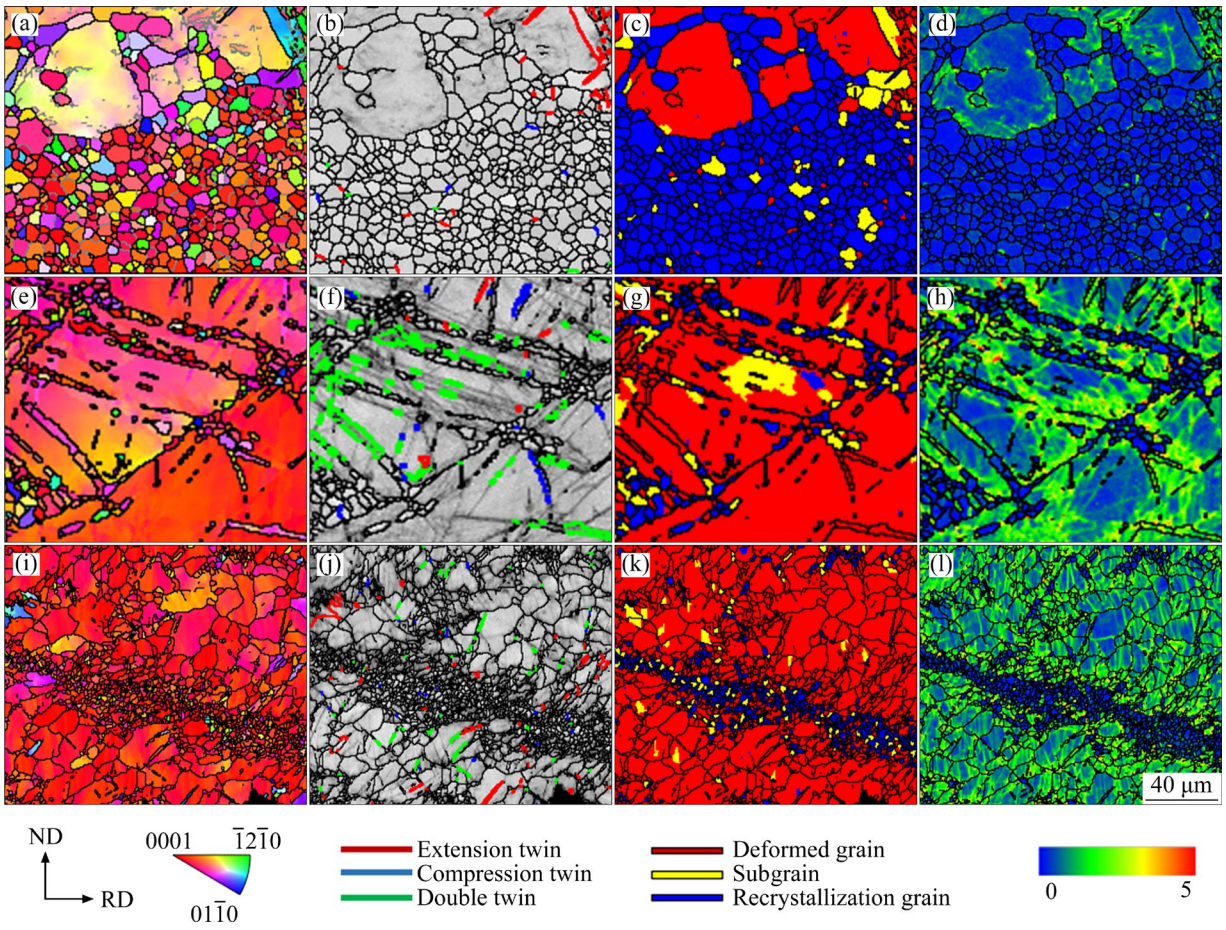

Fig. 6 EBSD analysis results of rolled AZ31 sheets with different initial states: (a) Grain orientation map of AE sheet; (b−d) Twin distribution, recrystallization distribution and KAM map of AE sheet, respectively; (e) Grain orientation map of AC sheet; (f−h) Twin distribution, recrystallization distribution and KAM map of AC sheet, respectively; (i) Grain orientation map of AR sheet; (j−l) Twin distribution, recrystallization distribution and KAM maps of AR sheet, respectively

3.3 Macro-textures

Figure 7 shows the macro-textures of AZ31 alloy sheets with different initial states before and after rolling. Before rolling, it is found that the AE sheet exhibits the double-peak texture along the RD, as well as the texture with the *C*-axis of some grains parallel to the TD. After rolling, the texture transforms from the double-peak to the single peak, and the texture in the TD direction also disappears. The maximum texture intensity of AE sheet decreases from 5.570 to 3.974 MRD. For the AC sheet, there is a common scattered texture component before rolling, and the scattered texture component tilts towards the center after rolling, which is similar to the findings reported by WANG et al [20]. While the AR sheet exhibits a strong basal texture component before rolling and subsequently keeps the texture component after rolling, the maximum texture intensity slightly increases from 11.282 to 12.438 MRD.

3.4 Micro-cracks of AC and AR rolled sheets

To further analyze the crack initiation in the AC rolled sheet, the IPF, recrystallization, KAM and twins distribution maps of micro-cracks are shown in Fig. 8. It can be found that the micro-crack is initiated inside the local region where randomly oriented fine grains are present, as depicted in Fig. 8(a). These fine grains have been proven to be recrystallized grains. Compared with the surrounding coarse grains containing high density dislocations, most of the dislocations are consumed within the local fine-grained region (Fig. 8(d)). Meanwhile, the micro-crack inside a coarse grain can also be found in Fig. 8(e), and profuse twins are formed around the micro-crack.

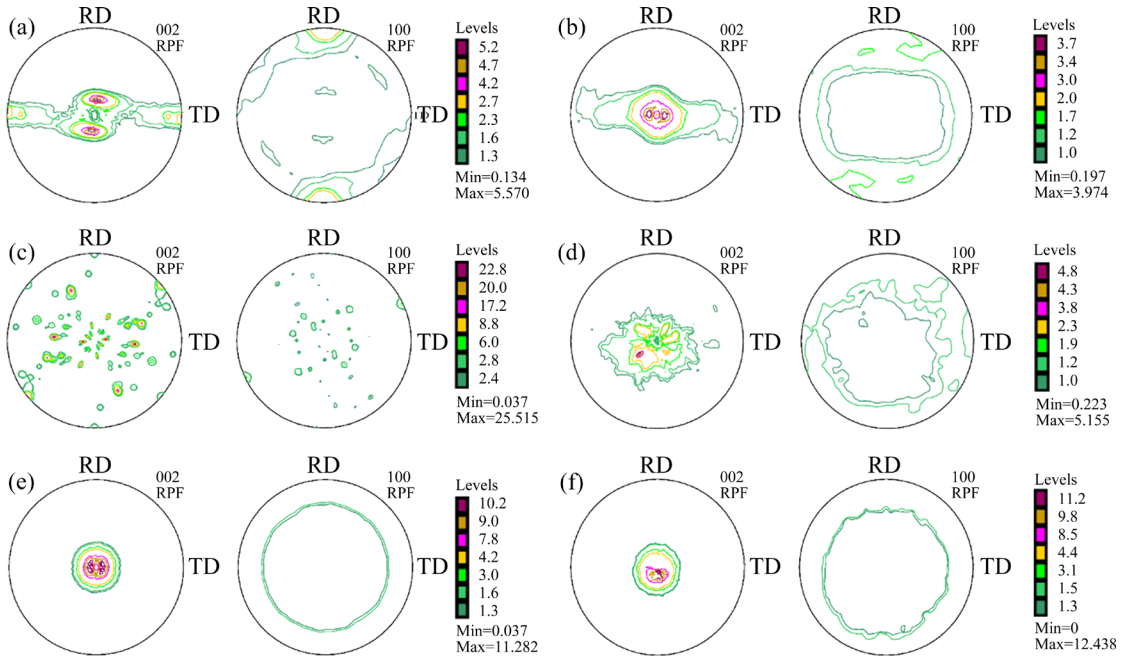

Fig. 7 Macro-textures at edge of AZ31 sheets with different initial states: (a, c, e) Textures of AE, AC and AR sheets before rolling, respectively; (b, d, f) Textures of AE, AC and AR sheets after rolling, respectively

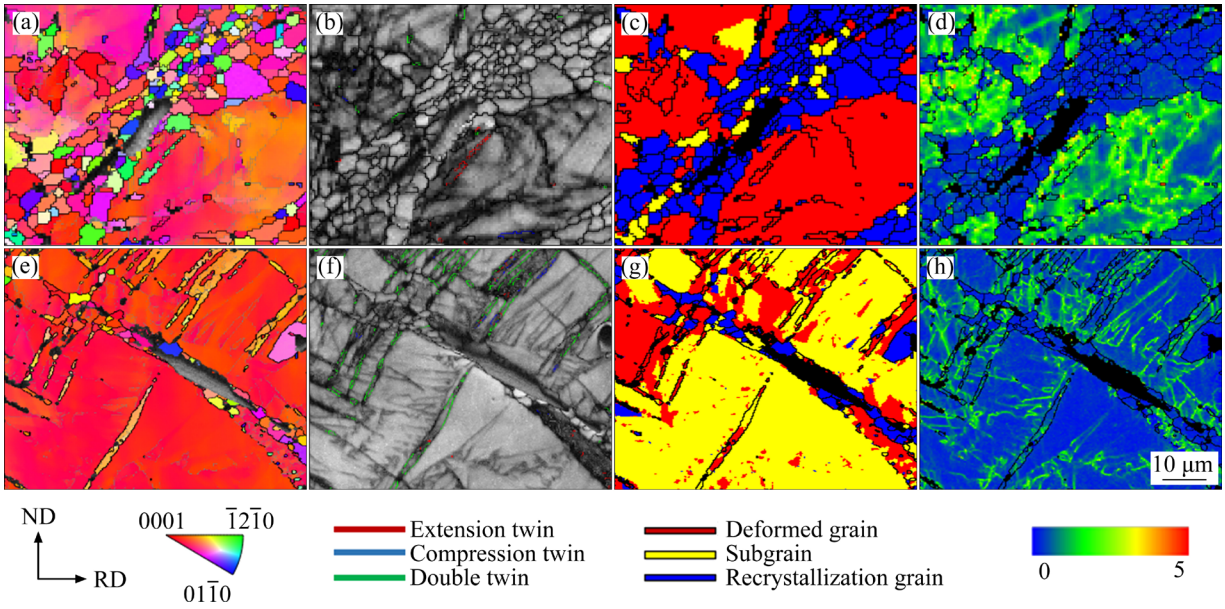

Fig. 8 Microstructures of two micro-cracks in AC AZ31 sheets after rolling: (a, e) Grain orientation maps of two different micro-cracks; (b−d) Twin distribution, recrystallization distribution and KAM maps in (a), respectively; (f−h) Twin distribution, recrystallization distribution and KAM maps in (e), respectively

According to the twin distribution map in Fig. 8(f), these twins are determined as double twins. Further observation shows that the micro-crack is located inside the twin where recrystallization has occurred, typically referred to as twin-induced recrystallization (TDRX), as shown in Fig. 8(g).

Figure 9 shows the local microstructure containing the micro-crack of AR sheets after rolling. The micro-crack is initiated inside the shear band, which is composed of the fine DRXed grains (Figs. 9(b−d)). To analyze the propagation of the micro-crack initiated inside the shear band, the microstructures of the typical penetrating crack on the RD−ND section of AR sheet after rolling is shown in Fig. 10. It is evident that the grains at the crack boundary are fine recrystallized grains, which

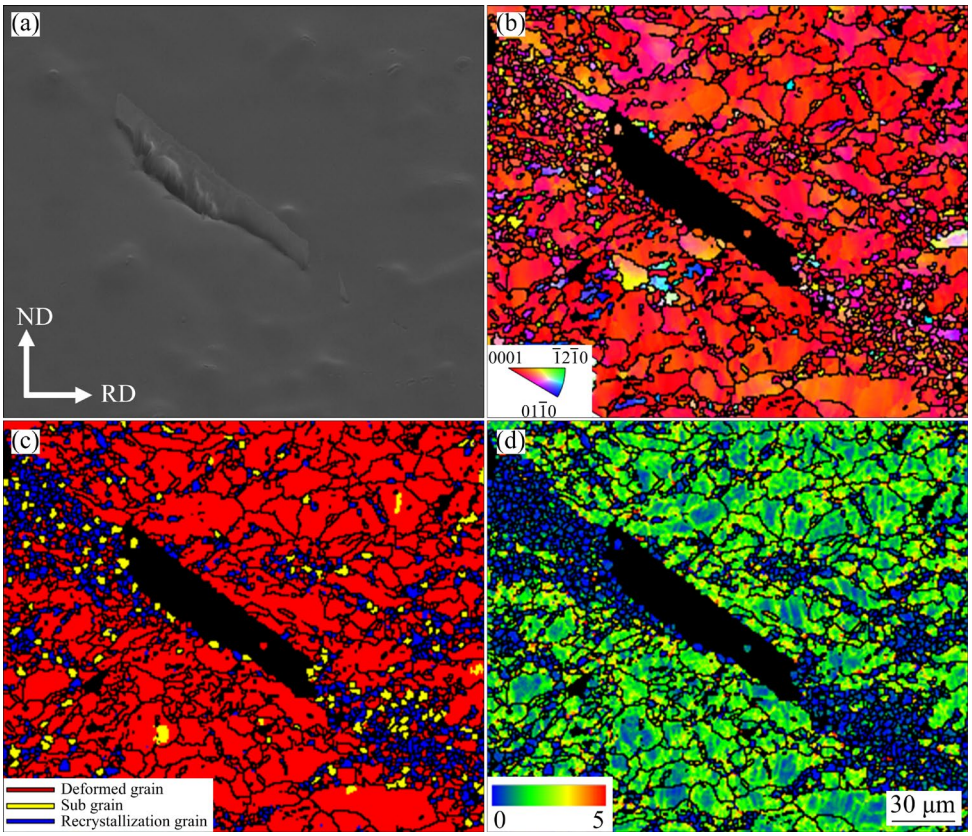

Fig. 9 Local microstructures with micro-cracks of AR AZ31 sheets after rolling: (a) Micro-cracks; (b−d) Grain orientation map, recrystallization distribution and KAM map, respectively

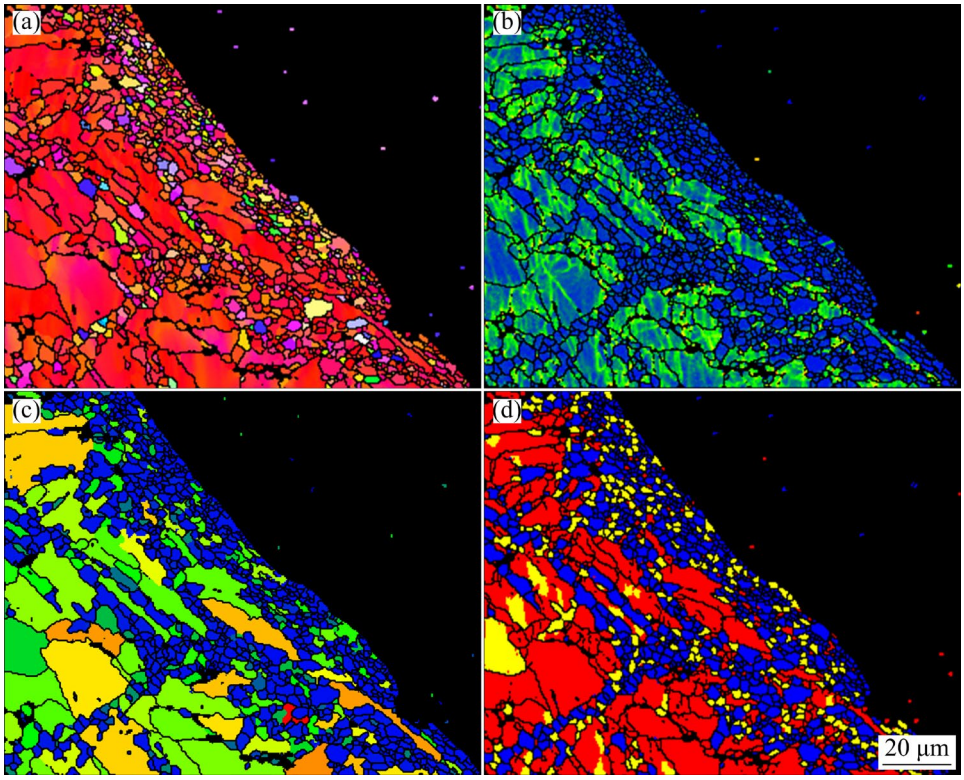

Fig. 10 Microstructures of penetrated crack edge on longitudinal section of AR AZ31 sheets after rolling: (a) Grain orientation map; (b) Recrystallization distribution; (c) KAM map; (d) GOS map

obviously have lower dislocation density and grain orientation spread (GOS) than those further away from the crack boundary (Fig. 10(d)). Apparently, this indicates that the micro-crack mainly propagates along the fine-grained shear bands and eventually penetrates the RD−ND section to form large cracks. This is in agreement with the work of HUANG et al [21].

4 Discussion

4.1 Effect of texture on edge crack behavior during hot rolling

In general, the texture has a significant impact on the rolling formability of the Mg sheet, which in turn affects the edge cracking behavior. As shown in Fig. 3, the initial sheets with different states exhibit varying edge cracking behaviors after the same online heating rolling process. This is probably related to the initial texture of rolled sheets. The middle texture component of the AE sheet shows an obvious double-peak characteristic with a tilt towards the RD before rolling, as illustrated in Fig. 7(a). This texture is beneficial to the plastic deformation of the sheet along the RD, thereby enhancing the rollability of the AE sheet. A similar report can be observed in the studies by GUO et al [22] and HAN et al [23]. Meanwhile, the texture consisting of TD-oriented grains in the AE sheet is prone to activating prismatic slip under high temperatures. This further coordinates the deformation, leading to excellent rollability and subsequent suppression of edge cracking. CHUN and DAVIES [24] also reported the favorable activation of prismatic $\langle a \rangle$ slip during the rolling of the TB plate, where the *C*-axis of grains is parallel to the TD. Therefore, there are no obvious edge cracks in the AE rolled sheet. Mg sheets with a strong basal texture can deteriorate their formability and easily result in the formation of edge cracks. HUANG et al [25] investigated the effect of initial texture on the deep-draw ability of AZ31 alloy sheets. They found a lower drawing ratio for the sheet with a stronger basal texture, which exhibited poorer formability. While a strong basal texture is evident at the edge of the AR sheet before rolling, a large number of edge cracks are generated in the AR sheets after rolling. The AC sheet has a commonly scattered texture component before rolling, and severe edge cracking behavior still occurs. This indicates that the edge crack behavior is also affected by other factors, such as the coarse second particles mentioned above, as well as the microstructure, which will be discussed in the next section.

4.2 Effect of microstructure on crack initiation during hot rolling

As shown in Fig. 6, the degree of the recrystallization in the AE rolled sheet is obviously higher than that in the AC and AR rolled sheets. GUO et al [7] reported that recrystallization (DRX) was an effective method for consuming strain energy. Therefore, the higher degree of DRX could release more rolling strain. This leads to a higher strain accommodation limitation in the AE rolled sheet. Additionally, a relatively uniform microstructure is also obtained in the AE rolled sheet due to the higher DRX, resulting in better deformability and thereby inhibiting the initiation of edge cracks. While both the AC and AR sheets exhibit extremely uneven microstructure after rolling, this is mainly due to strain localization in the plastic deformation caused by lower recrystallization. This type of non-uniform microstructure has a poor coordination deformation ability and might be considered as the main factor for inducing the cracking [26]. Therefore, it can be concluded that the AE sheet shows better online heating rollability and is less prone to cracking than the AC and AR sheets during the same rolling process in this work.

4.3 Mechanism of crack initiation during hot rolling

As shown in Figs. 4(d) and (e), micro-cracks are initiated inside the local fine-grained regions of both the AC and AR rolled sheets. This indicates that local fine recrystallization grains play an important role in acting as the initiation site for micro-cracks under high rolling forces. This is in agreement with the work of GUO et al [12]. When the sheet is deformed at high temperatures, active atomic diffusion will occur at the grain boundaries, leading to the formation of defects such as micro-voids. In this case, more grain boundaries due to grain refinement may lead to the generation of more micro-void defects. ZHU et al [27] reported that the number of micro-voids and defects at the grain boundaries increases with the decrease of grain boundary size, due to the larger proportion of

grain boundaries. In addition, the fine-grained area can be regarded as a flow softening region due to dynamic recrystallization, which can easily lead to plastic instability. Therefore, the local fine-grained regions are more unstable under deformation at high temperatures, which further accelerates the initiation of micro-cracks. And the DRXed fine-grained area tends to absorb subsequent plastic strain during rolling. JIA et al [28] pointed out that the plastic deformation was mainly concentrated in shear deformation fine-grained bands. The grain size of the local DRX fine-grained regions in the AC and AR rolled sheets is less than 5 μm, which may induce an additional deformation mechanism of grain boundary sliding (GBS) at an appropriate strain rate [29]. This can also lead to a considerable plastic strain concentration within the fine-grained region.

On the one hand, the initiation of cracks in the fine-grained region depends on whether the critical strain is reached [30,31]. On the other hand, the absorbed deformation in the fine-grained area may be further localized and produce some dislocations in a local area, leading to local stress concentration. Consequently, some micro-voids might be initiated due to the accumulation of dislocations at local triple junctions. LIU et al [32] also detected the voids and micro-cracks at grain triple junctions in a thin layer of recrystallized grains, and these voids finally lead to the formation of the micro-cracks. In addition, the micro-cracks can also be observed inside the twin in the AC rolled sheet, as shown in Fig. 8(e). Many double twins are formed around the micro-cracks (Fig. 8(f)), indicating that this coarse parent grain orientation is conducive to this twin type. Therefore, it seems that this DRX is probably induced inside the double twins. KIM et al [33] found that a large number of dislocations were generated inside the double twins through TEM, which provided the driving force for the DRX.

It is reported that there is a competitive role between crack initiation and DRX, which is determined by the ratio of σ_c/σ_D, where σ_c and σ_D represent the critical stress against the nucleation of micro-cracks and the occurrence of DRX, respectively [32]. DRX is most likely to occur initially in some twins and reduce the dislocation density inside twin lamellae. However, the concentrated stress caused by the accumulation of dislocations inside the twins is significant in this work. The extent of DRX cannot release enough strain energy, and then the crack initiation along the grain boundary releases the remaining energy, which eventually leads to the formation of micro-cracks. In addition, the strain between the original coarse grain and small recrystallized grains is incompatible, which can provide the driving force for the interface crack, and eventually leading to the nucleation and propagation of the micro-cracks.

5 Conclusions

(1) The AR rolled sheet exhibits the severest edge cracking, which is caused by a strong basal texture and an extremely uneven microstructure with shear bands. While no visible edge cracks occur in the AE sheet due to the tilted texture and more uniform deformation during rolling.

(2) In the AC rolled sheet, due to strain incompatibility and significant stress concentration, micro-cracks are mainly initiated inside the local fine-grained area and inside the twins where the twin-induced recrystallization occurs.

(3) The shear bands of fine-grained also act as the main crack initiation source in the AR rolled sheet due to the relative instability of fine-grained boundaries, and finally the micro-cracks expand into large edge cracks along the shear band.

CRediT authorship contribution statement

Qiu-yan SHEN: Formal analysis, Investigation, Resources, Data curation, Writing − Original draft; **Shang-yi ZHANG:** Visualization; **Qiang LIU:** Conceptualization, Methodology; **Jiang-feng SONG:** Supervision, Project administration, Funding acquisition, Writing − Review & editing; **Dong-xia XIANG:** Supervision; **Bin JIANG** and **Fu-sheng PAN:** Project administration, Funding acquisition.

Declaration of competing interest

The authors declare that they have no known competing financial interests or personal relationships that could have appeared to influence the work reported in this paper.

Acknowledgments

This work was financially supported by the National Natural Science Foundation of China (Nos. 52071036, U2037601), the Guangdong Major Project of Basic and Applied Basic Research, China (No. 2020B0301030006),

the Independent Research Project of State Key Laboratory of Mechanical Transmissions, China (Nos. SKLMT-ZZKT-2022Z01, SKLMT-ZZKT-2022M12), and the Chongqing Science and Technology Commission, China (No. CSTB2022TIAD-KPX0021).

References

[1] SONG Jiang-feng, CHEN Jing, XIONG Xiao-ming, PENG Xiao-dong, CHEN Dao-lun, PAN Fu-sheng. Research advances of magnesium and magnesium alloys worldwide in 2021 [J]. Journal of Magnesium and Alloys, 2022, 10: 863−898.

[2] MO Ning, TAN Qi-yang, BERMINGHAM M, HUANG Yuan-ding, DIERINGA H, HORT N, ZHANG Ming-xing. Current development of creep-resistant magnesium cast alloys: A review [J]. Materials & Design, 2018, 155: 422−442.

[3] NAZEER F, LONG Jian-yu, YANG Zhe, LI Chuan. Superplastic deformation behavior of Mg alloys: A review [J]. Journal of Magnesium and Alloys, 2022, 10: 97−109.

[4] JIN Zhong-zheng, ZHA Min, WANG Si-qing, WANG Shi-chao, WANG Cheng, JIA Hai-long, WANG Hui-yuan. Alloying design and microstructural control strategies towards developing Mg alloys with enhanced ductility [J]. Journal of Magnesium and Alloys, 2022, 10: 1191−1206.

[5] JIA Wei-tao, TANG Yan, NING Fang-kun, LE Qi-chi, BAO Lei. Optimum rolling speed and relevant temperature- and reduction-dependent interfacial friction behavior during the break-down rolling of AZ31B alloy [J]. Journal of Materials Science & Technology, 2018, 34: 2051−2062.

[6] DING Yun-peng, LE Qi-chi, ZHANG Zhi-giang, CUI Jian-zhong. Effects of the heavy reduction rolling on the microstructure and edge crack of casted magnesium alloys [J]. Journal of Northeastern University (Natural Science), 2014, 35: 379−383.

[7] GUO Fei, ZHANG Ding-fei, YANG Xu-sheng, JIANG Lu-yao, CHAI Sen-sen, PAN Fu-sheng. Influence of rolling speed on microstructure and mechanical properties of AZ31 Mg alloy rolled by large strain hot rolling [J]. Materials Science and Engineering: A, 2014, 607: 383−389.

[8] TIAN Jing, LU Hui-hu, ZHANG Wang-gang, NIE Hui-hui, SHI Quan-xin, DENG Jia-fei, LIANG Wei, WANG Li-fei. An effective rolling process of magnesium alloys for suppressing edge cracks: Width-limited rolling [J]. Journal of Magnesium and Alloys, 2022, 10: 2193−2207.

[9] JI Ya-feng, DUAN Jin-rui, LI Hua-ying, LIU Yuan-ming, PENG Wen, MA Li-feng. Improvement of edge crack damage of magnesium alloy by optimizing the edge curve during cross variable thickness rolling [J]. The International Journal of Advanced Manufacturing Technology, 2021, 112: 1993−2002.

[10] LIU Qiang, SONG Jiang-feng, ZHAO Hua, XIAO Bi-quan, ZHENG Xiao-jian, PAN Fu-sheng. Improved edge quality for AZ31 sheets using online heating rolling technique [J]. Journal of Materials Engineering and Performance, 2020, 29: 4212−4221.

[11] PEI Ri-sheng, KORTE-KERZEL S, AL-SAMMAN T. The role of mesoscopic deformation heterogeneities in plastic flow and recrystallization of a magnesium sheet alloy [J]. Materialia, 2020, 12: 100715.

[12] GUO Fei, ZHANG Ding-fei, FAN Xiao-wei, JIANG Lu-yao, YU Da-liang, PAN Fu-sheng. Deformation behavior of AZ31 Mg alloys sheet during large strain hot rolling process: A study on microstructure and texture evolutions of an intermediate-rolled sheet [J]. Journal of Alloys and Compounds, 2016, 663: 140−147.

[13] SHANG L, JUNG I H, YUE S, VERMA R, ESSADIQI E. An investigation of formation of second phases in microalloyed, AZ31 Mg alloys with Ca, Sr and Ce [J]. Journal of Alloys and Compounds, 2010, 492: 173−183.

[14] GO J B, LEE J U, MOON B G, YOON J H, PARK S H. Improvement in mechanical properties of rolled AZ31 alloy through combined addition of Ca and Gd [J]. Metals and Materials International, 2020, 26: 1779−1785.

[15] BAEK S M, PARK H K, YOON J I, JUNG J, MOON J H, LEE S G, KIM J H, KIM T S, LEE S, KIM N J, KIM H S. Effect of secondary phase particles on the tensile behavior of Mg−Zn−Ca alloy [J]. Materials Science and Engineering: A, 2018, 735: 288−294.

[16] XIAO Bi-quan, SONG Jiang-feng, TANG Ai-tao, JIANG Bin, SUN Wen-yan, LIU Qiang, ZHAO Hua, PAN Fu-sheng. Effect of pass reduction on distribution of shear bands and mechanical properties of AZ31B alloy sheets prepared by on-line heating rolling [J]. Journal of Materials Processing Technology, 2020, 280: 116611.

[17] RAO Xi-xin, WU Yun-peng, PEI Xiao-dong, JING Yu-hai, LUO Lan, LIU Yong, LU Jian. Influence of rolling temperature on microstructural evolution and mechanical behavior of AZ31 alloy with accumulative roll bonding [J]. Materials Science and Engineering: A, 2019, 754: 112−120.

[18] WANG Yan-nan, XIN Yun-chang, YU Hui-hui, LV Liang-chen, LIU Qing. Formation and microstructure of shear bands during hot rolling of a Mg−6Zn−0.5Zr alloy plate with a basal texture [J]. Journal of Alloys and Compounds, 2015, 644: 147−154.

[19] FATEMI-VARZANEH S M, ZAREI-HANZAKI A, CABRERA J M. Shear banding phenomenon during severe plastic deformation of an AZ31 magnesium alloy [J]. Journal of Alloys and Compounds, 2011, 509: 3806−3810.

[20] WANG Hui-yuan, ZHANG En-bo, NAN Xiao-long, ZHANG Lei, GUAN Zhi-ping, JIANG Qi-chuan. A comparison of microstructure and mechanical properties of Mg−9Al−1Zn sheets rolled from as-cast, cast-rolling and as-extruded alloys [J]. Materials & Design, 2016, 89: 167−172.

[21] HUANG X S, SUZUKI K, WATAZU A, SHIGEMATSU I, SAITO N. Microstructural and textural evolution of AZ31 magnesium alloy during differential speed rolling [J]. Journal of Alloys and Compounds, 2009, 479: 726−731.

[22] GUO Fei, ZHANG Ding-fei, YANG Xu-sheng, JIANG Lu-yao, PAN Fu-sheng. Microstructure and texture evolution of AZ31 magnesium alloy during large strain hot rolling [J]. Transactions of Nonferrous Metals Society of China, 2015, 25: 14−21.

[23] HAN Ting-zhuang, HUANG Guang-sheng, DENG Qian-yuan, WANG Guan-gang, JIANG Bin, TANG Ai-tao, ZHU Yun-tian, PAN Fu-sheng. Grain refining and mechanical properties of AZ31 alloy processed by accumulated extrusion bonding [J]. Journal of Alloys and Compounds, 2018, 745: 599−608.
[24] CHUN Y B, DAVIES C H J. Texture effects on development of shear bands in rolled AZ31 alloy [J]. Materials Science and Engineering: A, 2012, 556: 253−259.
[25] HUANG Xin-sheng, SUZUKI K, CHINO Y, MABUCHI M. Influence of initial texture on cold deep drawability of Mg−3Al−1Zn alloy sheets [J]. Materials Science and Engineering: A, 2013, 565: 359−372.
[26] SABOKPA O, ZAREI-HANZAKI A, ABEDI H R. An investigation into the hot ductility behavior of AZ81 magnesium alloy [J]. Materials Science and Engineering: A, 2012, 550: 31−38.
[27] ZHU Qiang, WANG Chuan-jie, QIN He-yong, CHEN Gang, ZHANG Peng. Effect of the grain size on the microtensile deformation and fracture behaviors of a nickel-based superalloy via EBSD and in-situ synchrotron radiation X-ray tomography [J]. Materials Characterization, 2019, 156: 109875.
[28] JIA Wei-tao, MA Li-feng, LE Qi-chi, ZHI Chen-chen, LIU Peng-tao. Deformation and fracture behaviors of AZ31B Mg alloy at elevated temperature under uniaxial compression [J]. Journal of Alloys and Compounds, 2019, 783: 863−876.
[29] KIM H L, CHANG Y W. Deformation mechanism temperature-dependence of AZ31 magnesium alloy [J]. Metals and Materials International, 2011, 17: 563.
[30] KUANG Jie, LI Xiao-hui, ZHANG Rui-kun, YE Yong-da, LUO A A, TANG Guo-yi. Enhanced rollability of Mg_3Al_1Zn alloy by pulsed electric current: A comparative study [J]. Materials & Design, 2016, 100: 204−216.
[31] ZHAO Chen-chen, WANG Tao, LI Zi-xuan, LIU Jiang-lin, HUANG Zhi-quan, HUANG Qing-xue. Prediction of magnesium alloy edge crack in edge-constraint rolling process by using a modified GTN model [J]. International Journal of Mechanical Sciences, 2023, 241: 107961.
[32] LIU X, ZHU B W, XIE C, ZHANG J, TANG C P, CHEN Y Q. Twinning, dynamic recrystallization, and crack in AZ31 magnesium alloy during high strain rate plane strain compression across a wide temperature [J]. Materials Science and Engineering: A, 2018, 733: 98−107.
[33] KIM H L, LEE J H, LEE C S, BANG W, AHN S H, CHANG Y W. Shear band formation during hot compression of AZ31 Mg alloy sheets [J]. Materials Science and Engineering: A, 2012, 558: 431−438.

铸态、轧制态和挤压态 Mg−3Al−1Zn 薄板边裂行为的比较

沈秋燕[1,2]，张上一[1,2]，刘 强[1,2]，宋江凤[1,2,3]，向冬霞[4]，蒋 斌[1,2,3]，潘复生[1,2,3]

1. 重庆大学 国家镁合金材料工程技术研究中心，重庆 400044；
2. 重庆大学 材料科学与工程学院，重庆 400044；
3. 重庆大学 先进铸造技术国家重点实验室，重庆 400044；
4. 重庆先进轻金属研究院，重庆 400044

摘 要：边裂是镁合金板材在轧制过程中出现最严重的问题之一，它限制了镁合金板材的应用。本文系统地研究和比较了铸态(AC)、轧制态(AR)和挤压态(AE)不同初始态 AZ31 合金板材在轧制温度为 250 ℃、单道次压下率为 50%时在线加热轧制工艺下的边裂行为。结果表明，AC 和 AR 板材经在线加热轧制后均表现出严重的边裂行为。其中，AR 板材在轧制面(RD−TD)和纵截面(RD−ND)上表现出最严重的边裂行为，这是其强烈的基面织构和含有剪切带且极不均匀的显微组织所致。而 AE 轧制板材没有出现明显的边裂现象，这主要与轧制过程中织构倾斜和动态再结晶较多有关。此外，研究还发现 AC 轧制板材的微裂纹主要产生于局部细晶区和发生再结晶的孪晶内部，AR 轧制板材的微裂纹主要在剪切带内部扩展。同时，对 AC 和 AR 轧制板材的微裂纹萌生机理进行了探讨。

关键词：AZ31 板材；边裂行为；初始态；织构；显微组织

(Edited by Wei-ping CHEN)